BIOMOLECULES & THERAPEUTICS

Original Article
Biomol Ther 33(3), 438-446 (2025)

The SIRT6 Activator MDL-800 Inhibits PPARα and Fatty acid Oxidation-Related Gene Expression in Hepatocytes

Yeonsoo Kim, Hyeokjin Lim, Ye Eun Cho and Seonghwan Hwang*

College of Pharmacy and Research Institute for Drug Development, Pusan National University, Busan 46241, Republic of Korea

Abstract

A histone deacetylase SIRT6 regulates the transcription of various genes involved in lipid metabolism. Fatty acid (FA) oxidation plays a pivotal role in maintaining hepatic lipid homeostasis, and its dysregulation significantly contributes to lipotoxicity and inflammation, driving the progression of steatotic liver disease. While SIRT6 is known to activate peroxisome proliferator-activated receptor-alpha (PPARα), a central regulator of FA oxidation, the development of SIRT6 activators capable of enhancing FA oxidation and mitigating steatotic liver disease has yet to be achieved. This study evaluated the effect of MDL-800, a selective SIRT6 activator, on the expression of PPARα and genes related to FA oxidation. In AML12 mouse hepatocytes, MDL-800 treatment activated SIRT6 but unexpectedly decreased the expression of PPARα and its FA oxidation-associated target genes. Furthermore, OSS128167, a selective SIRT6 inhibitor, did not reverse the suppressive effects of MDL-800 on PPARα, suggesting that MDL-800 downregulates PPARα and FA oxidation-related genes through a mechanism independent of SIRT6 activation. Mechanistic investigations revealed that MDL-800 increased the production of reactive oxygen species and activated stress kinases. The inhibition of PPARα by MDL-800 was reversed by co-treatment with the antioxidant N-acetylcysteine or the JNK inhibitor SP600125. In summary, MDL-800 suppresses PPARα and FA oxidation-related genes primarily through the induction of oxidative stress in hepatocytes, independent of its role as a SIRT6 activator.

Key Words: MDL-800, SIRT6, Reactive oxygen species, Fatty acid oxidation, PPARα

INTRODUCTION

SIRT6 is a member of the sirtuin family that functions as a NAD-dependent histone deacetylase (You and Liang, 2023). By regulating the transcription of numerous genes, SIRT6 orchestrates a variety of biological processes associated with longevity, including metabolism, oxidative stress response, DNA repair, autophagy, and inflammation (Jiang *et al*., 2013; You and Liang, 2023). Accordingly, SIRT6 has been identified as a protective factor against aging-related conditions, such as metabolic disease and cancer (Tasselli *et al*., 2017).

The involvement of SIRT6 in hepatic lipid synthesis and metabolism is well-documented. The biosynthesis of fatty acids (FAs) and triglycerides from carbohydrates is regulated by several transcription factors, such as liver X receptor (LXR), carbohydrate response element binding protein (ChREBP), and sterol regulatory element binding protein-1 (SREBP1) (Schultz *et al*., 2000; Cha and Repa, 2007; Xu *et al*., 2013). SIRT6 deacetylates these transcription factors, suppressing their activity and thus inhibiting lipid synthesis (Zhu *et al*., 2021). Additionally, SIRT6 plays a role in FA β-oxidation, a process that converts FAs into acetyl CoA for energy production. FA oxidation is catalyzed by multiple enzymes, such as carnitine palmitoyltransferase 1 (CPT1) and acyl-CoA oxidase 1 (ACOX1), whose transcription is activated by peroxisome proliferator-activated receptor-alpha (PPARα) (Moreno *et al*., 2010). SIRT6 directly interacts with and transactivates PPARα, thereby promoting the expression of FA oxidation-related genes (Naiman *et al*., 2019). In addition, SIRT6 represses microRNA-122, which targets genes involved in FA oxidation, such as ATP citrate lyase and CPT1 (Elhanati *et al*., 2016). These lines of evidence support the possibility that pharmacological activation of SIRT6 could inhibit hepatic lipogenesis and activate FA oxidation, thereby maintaining hepatic lipid homeostasis.

MDL-800 is a small-molecule activator of SIRT6, which binds to an allosteric site on SIRT6 and enhances its deacetylase activity, with an EC_{50} value of 10.3 μM (Huang *et al*.,

Open Access **https://doi.org/10.4062/biomolther.2024.251**

Received Dec 30, 2024 **Revised** Mar 2, 2025 **Accepted** Mar 4, 2025
Published Online Apr 4, 2025

***Corresponding Author**
E-mail: shhwang@pusan.ac.kr
Tel: +82-51-510-2817, Fax: +82-51-513-6754

2018). Since its discovery (Huang *et al*., 2018), MDL-800 has been shown to possess various biological activities. For instance, MDL-800 has demonstrated potential in inhibiting tumor growth. MDL-800 reduced the proliferation of hepatocellular carcinoma (HCC) through SIRT6-mediated cell-cycle arrest *in vitro* and ameliorated tumor growth in a xenograft model (Huang *et al*., 2018). MDL-800 also inhibited the proliferation of multiple non-small cell lung cancer cell lines in a SIRT6-dependent manner (Shang *et al*., 2021). Beyond cancer, MDL-800 has demonstrated benefits in non-malignant conditions. For example, MDL-800 was reported to inhibit liver fibrosis induced by carbon tetrachloride administration in mice (Zhang *et al*., 2021). Wu *et al*. demonstrated that MDL-800 attenuated heart failure in mice induced by high-fat diet feeding and streptozotocin treatment (Wu *et al*., 2022).

Metabolic dysfunction-associated steatotic liver disease (MASLD) is a spectrum of disease that ranges from steatosis to steatohepatitis, cirrhosis, and HCC (Sanyal, 2019; Mehal, 2023). MASLD has emerged as the leading cause of chronic liver disease, affecting approximately 38% of the adult population (Wong *et al*., 2023). Metabolic dysfunction impairs FA oxidation, leading to elevated hepatic levels of lipotoxic free FAs (Friedman *et al*., 2018). This lipotoxicity induces hepatocyte death, exacerbating the progression of simple steatosis to steatohepatitis with increased inflammation and fibrosis (Geng *et al*., 2021; Chung *et al*., 2022). Given the role of SIRT6 in regulating lipid synthesis and metabolism in the liver (Dong, 2023), modulating SIRT6 activity is hypothesized to affect MASLD pathogenesis. Indeed, hepatocyte-specific deletion of the *Sirt6* gene in mice enhanced steatosis by increasing FA synthesis and inhibiting FA oxidation (Kim *et al*., 2010). However, it has not been tested whether MDL-800, the first-in-class small-molecule SIRT6 activator (Huang *et al*., 2018), represses hepatic fat accumulation. In particular, the effect of MDL-800 on FA oxidation has not been reported although SIRT6 is known to activate PPARα and its downstream FA oxidation-related genes (Naiman *et al*., 2019).

In this study, we investigated the effects of MDL-800 on the expression of PPARα and FA oxidation-related genes in hepatocytes. In contrast to the established role of SIRT6 in activating PPARα, we observed that MDL-800 inhibits PPARα and FA oxidation-associated genes in a SIRT6-independent manner. Mechanistic studies revealed that MDL-800 suppresses PPARα and FA oxidation genes by producing reactive oxygen species (ROS) and activating stress kinases. SIRT6 is generally recognized for its protective role against cancer, and previous studies have shown that MDL-800 suppresses tumor growth via SIRT6-dependent mechanisms, such as cell cycle arrest (Huang *et al*., 2018). The current study expands the current understanding of the anti-proliferative properties of MDL-800 by demonstrating its ability to inhibit PPARα and FA oxidation through a SIRT6-independent mechanism. Given that FA oxidation provides energy essential for cancer cell survival and proliferation (Carracedo *et al*., 2013), the suppression of FA oxidation may contribute to reduced tumor growth. These findings provide new insights into the mechanisms underlying the anti-proliferative properties of MDL-800 reported in previous studies.

MATERIALS AND METHODS

Materials

MDL-800, N-acetylcysteine (NAC), and dexamethasone were procured from Sigma-Aldrich (St. Louis, MO, USA). OSS128167 and SP600125 were obtained from MedChemExpress (Monmouth Junction, NJ, USA). The mixture of insulin, transferrin, and selenium (ITS) was purchased from Thermo Fisher Scientific (Waltham, MA, USA). Fetal bovine serum was acquired from Hyclone (Logan, UT, USA). Penicillin-streptomycin was sourced from Welgene (Gyeongsan, Korea).

Cell culture and transient transfection

AML12 mouse hepatocytes were cultured in a 1:1 mixture of Dulbecco's Modified Eagle Medium (DMEM) and Ham's F12 medium (Welgene) containing 0.005 mg/mL insulin, 0.005 mg/mL transferrin, 5 ng/mL selenium, 40 ng/mL dexamethasone, 10% fetal bovine serum, and penicillin–streptomycin. T-75 flasks were used for cell propagation, and the experiments were performed in 6-, 12-, and 96-well plates. The cells were grown until 80% confluency was reached and split at least twice a week.

Overexpression of SIRT6 in AML12 cells was achieved by a transient transfection of the plasmid that expresses the mouse *Sirt6* coding sequence or pcDNA3.1 as a negative control (Moon *et al*., 2019; Shi *et al*., 2020). Transfection was performed using Lipofectamine 3000 (Thermo Fisher Scientific) according to the manufacturer's protocol.

Isolation of primary mouse hepatocytes

Primary mouse hepatocytes were isolated from C57BL/6J mice using a two-step collagenase perfusion technique as previously described (Hwang *et al*., 2020b). Briefly, mice were anesthetized, and the liver was perfused in situ via the portal vein with a calcium- and magnesium-free HEPES-buffered saline solution (pH 7.4) (Welgene) to remove blood, followed by a collagenase-containing digestion buffer. The liver was excised and dissociated by gentle mechanical disruption, and the resulting cell suspension was filtered through a 70 μm cell strainer. Hepatocytes were enriched by low-speed centrifugation at 50×g for 5 min and washed twice in Dulbecco's modified Eagle's medium supplemented with 10% fetal bovine serum, 1% penicillin-streptomycin. Primary mouse hepatocytes were cultured at 37°C under 5% CO_2 in DMEM (Hyclone), supplemented with 10% fetal bovine serum (FBS; Hyclone) and 1% penicillin-streptomycin (Welgene).

Cell lysis, subcellular fractionation, and immunoblot analysis

To obtain whole-cell lysates, cells were lysed in RIPA buffer (Enzynomics, Seongnam, Korea) containing a cocktail of protease and phosphatase inhibitors (GenDEPOT, Baker, TX, USA) according to the manufacturer's instructions. The subcellular fractionation of cells by differential centrifugation was performed, as previously described (Hwang *et al*., 2016). The lysate protein concentration was determined using a BCA kit (Thermo Fisher Scientific). Immunoblot analyses were performed, as previously described (Hwang *et al*., 2020a). Briefly, the protein extracts were loaded onto 6, 8, or 12% polyacrylamide gels and transferred to nitrocellulose membranes (Thermo Fisher Scientific). The protein bands were visualized

Table 1. Sequences for the primers used in RT-qPCR analysis

Target mRNA	Forward primer	Reverse primer
Ppara	AACATCGAGTGTCGAATATGTGG	CCGAATAGTTCGCCGAAAGAA
Cpt1a	AGATCAATCGGACCCTAGACAC	CAGCGAGTAGCGCATAGTCA
Acox1	TAACTTCCTCACTCGAAGCCA	AGTTCCATGACCCATCTCTGTC
Lpin1	CTCCGCTCCCGAGAGAAAG	TCATGTGCAAATCCACGGACT
Ppargc1a	TATGGAGTGACATAGAGTGTGCT	CCACTTCAATCCACCCAGAAAG
Sirt6	ATGTCGGTGAATTATGCAGCA	GCTGGAGGACTGCCACATTA
Hmox1	AGGTACACATCCAAGCCGAGA	CATCACCAGCTTAAAGCCTTCT
Nqo1	AGGATGGGAGGTACTCGAATC	AGGCGTCCTTCCTTATATGCTA
Acadvl	CTACTGTGCTTCAGGGACAAC	CAAAGGACTTCGATTCTGCCC

using Pierce ECL Western Blotting Substrate (Thermo Fisher Scientific) and analyzed using a ChemiDocTM MP Imaging System (Bio-Rad, Hercules, CA, USA). The antibody against PPARα was obtained from Novus Biologicals (Littleton, CO, USA). Antibodies against LIPIN-1, acetyl-Histone H3 (Lys9), acetyl-Histone H3 (Lys56), SIRT6, JNK, phospho-JNK, ERK, phospho-ERK, p38, and phospho-p38 were purchased from Cell Signaling Technology (Danvers, MA, USA). The antibody against β-Actin was obtained from Santa Cruz Biotechnology (Dallas, TX, USA). The antibody against Lamin A/C was purchased from Abcam (Cambridge, MA, USA).

Total RNA isolation and RT-qPCR

Total RNA was purified from the cell cultures using Ribo-Ex™ reagents (Geneall, Seoul, Korea) as described previously (Kwon *et al*., 2024). Briefly, one microgram of RNA was reverse transcribed into complementary DNA (cDNA) using a SuPrimeScript cDNA Reverse Transcription Kit (GenetBio, Daejeon, Korea). cDNAs were amplified using a SYBR Green Kit (Enzynomics, Daejeon, Korea) on a CFX Connect Real-Time PCR System (Bio-Rad). The $2^{-\Delta\Delta Ct}$ method was used to calculate mRNA levels. The primer sequences used for PCR are listed in Table1.

Cell counting kit-8 (CCK-8) assay

Cell viability was measured using a CCK-8 assay kit (Dojindo, Kumamoto, Japan) according to the manufacturer's instructions (Cho *et al*., 2023). Briefly, AML12 mouse hepatocytes were treated with MDL-800 for 12 h. After the treatment period, the cells were further incubated with CCK-8 reagent for 90 min, and the absorbance was measured at 450 nm using a microplate reader.

DCF-DA assay

The production of intracellular ROS was measured using the 2',7'-dichlorofluorescin diacetate (DCF-DA) assay (Abcam, ab113851) (Hwang *et al*., 2020a). For fluorescence microscopy, cells were seeded in 6-well plates and cultured until 70-80% confluency. The cells were washed twice with pre-warmed phosphate-buffered saline (PBS) and incubated with 10 μM DCF-DA in serum-free medium for 30 min at 37°C in the dark. Following incubation, the cells were washed three times with PBS to remove excess probes and imaged using a fluorescence microscope (excitation/emission: 485/535 nm). For fluorescence measurement using a plate reader, cells were seeded in black 96-well plates and grown to 80% confluency. After washing with PBS, cells were incubated with 10 μM DCF-DA in serum-free medium for 30 min at 37°C in the dark. Excess dye was removed by washing three times with PBS, and fluorescence was measured immediately using a microplate reader (excitation/emission: 485/535 nm). Both data were expressed as mean ± standard error of the mean (SEM).

Statistical analysis

Data are expressed as the mean ± SEM and were analyzed using GraphPad Prism software (v.7.0a; GraphPad Software, La Jolla, CA, USA). Student's *t*-test were performed to compare the values obtained from the two groups. To compare more than three groups, a one-way analysis of variance was conducted, followed by post-hoc Tukey's tests to determine specific group differences. A *p*-value of <0.05 was deemed statistically significant.

RESULTS

MDL-800 inhibits the expression of PPARα and the downstream FA oxidation-related genes in hepatocytes

Previous studies have reported that MDL-800 (Fig. 1A) activates SIRT6 at concentrations above 25 μM in HCC cell lines (Huang *et al*., 2018), whereas lower concentrations of MDL-800 (5 and 10 μM) did not induce SIRT6 activation in AML12 mouse hepatocytes (Supplementary Fig. 1). Based on these findings, we examined the effects of MDL-800 at 25, 50, and 100 μM on the expression of FA oxidation-related genes. Treatment with MDL-800 at 50 and 100 μM significantly reduced PPARα expression in AML12 cells (Fig. 1B). Additionally, MDL-800 suppressed the expression of LIPIN-1, a coactivator that enhances PPARα by enhancing its interaction with PGC-1α (Finck *et al*., 2006). Acetylated histone H3K56 levels were reduced in MDL-800-treated cells, indicating that MDL-800 treatment activated SIRT6. As PPARα is a crucial transcription factor that controls the transcription of multiple FA oxidation-related genes, we further tested the effect of MDL-800 on the nuclear expression of PPARα. Nuclear levels of PPARα were reduced by a treatment with MDL-800 (Fig. 1C). Moreover, the mRNA levels of *Ppara* and FA oxidation-related genes, such as *Cpt1a*, *Acox1*, and *Lpin1*, were reduced by a treatment with MDL-800 in AML12 cells (Fig. 1D). These results indicate that MDL-800 suppresses PPARα and its downstream target genes involved in FA oxidation.

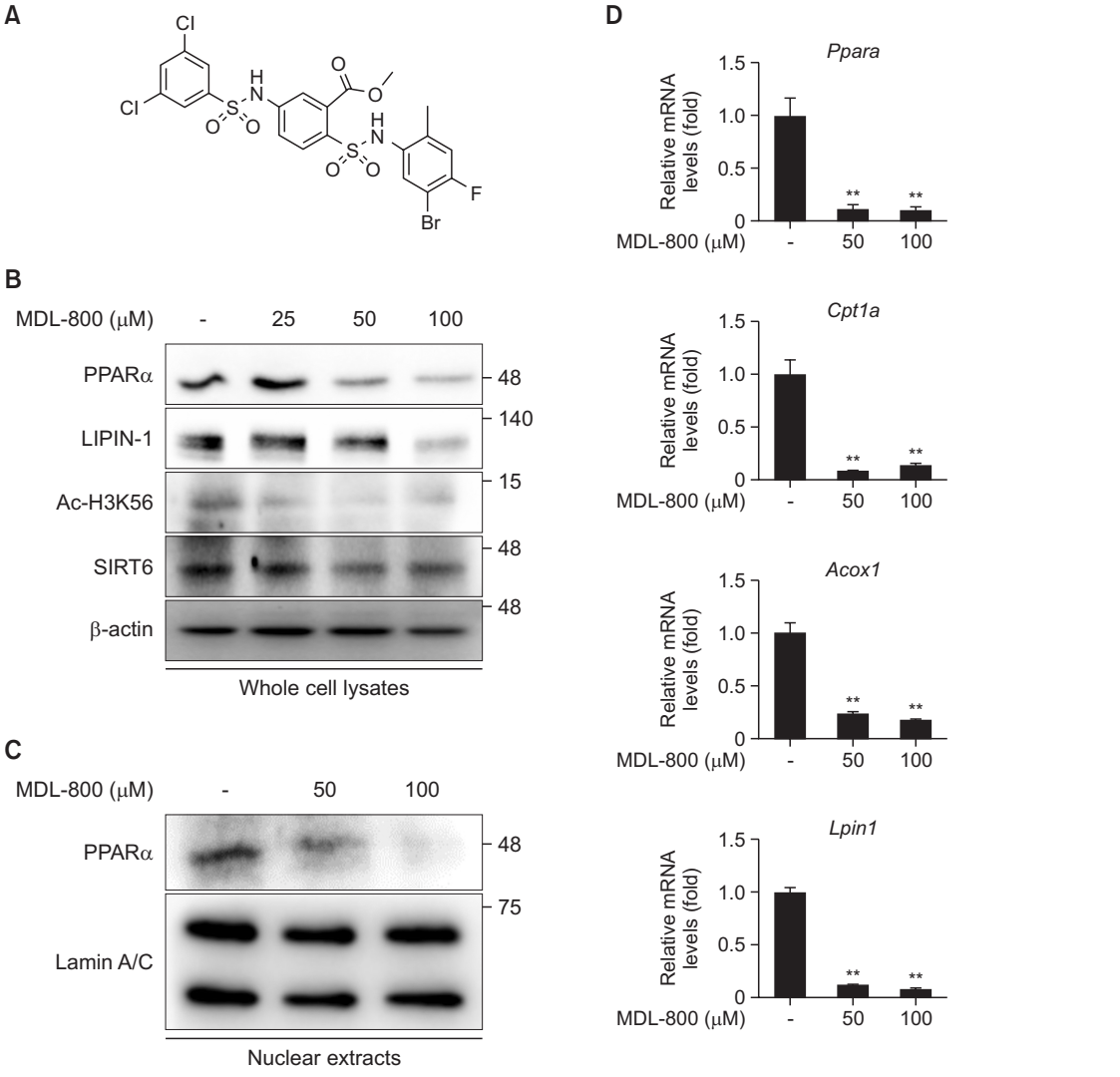

Fig. 1. MDL-800 inhibits the expression of PPARα and FA oxidation-related genes in AML12 cells. (A) Chemical structure of MDL-800. (B) AML12 mouse hepatocytes were treated with MDL-800 at concentrations of 25, 50, and 100 μM for 12 h. Whole cell lysates were subjected to immunoblot analyses of PPARα, LIPIN-1, acetylated histone H3K56, and SIRT6. (C, D) AML12 cells were treated with MDL-800 (50 and 100 μM) for 12 h. Nuclear extracts were subjected to immunoblot analyses for PPARα expression (panel C), and RNA was extracted for RT-qPCR analysis of *Ppara* and FA oxidation-related genes (panel D). Values represent the mean ± SEM (n=3). Statistical evaluations were performed using Student's *t*-test (**p<0.01).

MDL-800 inhibits FA oxidation-related genes in a SIRT6-independent manner

We investigated whether the inhibitory effects of MDL-800 on PPARα and FA oxidation-related genes are mediated by SIRT6 activation. Immunoblot analyses revealed that MDL-800 retained its ability to suppress PPARα and LIPIN-1 in the presence of OSS128167, a selective SIRT6 inhibitor (Fig. 2A). Consistently, OSS128167 treatment failed to reverse the reduction in *Ppara*, *Cpt1a*, and *Acox1* mRNA levels caused by MDL-800 in AML12 cells (Fig. 2B). These results indicate that MDL-800 inhibits PPARα and FA oxidation-related genes independently of SIRT6 activation. However, as expected, SIRT6 overexpression increased the mRNA levels of *Ppara*, *Cpt1a*, and *Ppargc1a* (encoding PGC-1α) in AML12 cells (Fig. 2C), in contrast to their downregulation by MDL-800 (Fig. 1D). Taken together, these results confirm that MDL-800 inhibits FA oxidation-related genes through a mechanism that is not dependent on SIRT6 activation.

MDL-800 induces cellular stress in hepatocytes

It has been reported that PPARα is inhibited by cellular stress involving the activation of stress kinases, such as JNK (Vernia *et al*., 2014). To elucidate the mechanism by which MDL-800 inhibits PPARα, we examined whether MDL-800 induces cellular stress at the identical concentrations that inhibit PPARα. MDL-800 treatment marginally caused cytotoxicity at 25 μM, and cytotoxicity was markedly enhanced at 50 and 100 μM (Fig. 3A). Treatment with 50 and 100 μM of MDL-800 remarkably increased the phosphorylation of JNK, p38, and ERK in AML12 cells (Fig. 3B). These results indicate that MDL-800 induces cytotoxicity and activates stress kinases, which may contribute to its inhibitory effects on PPARα.

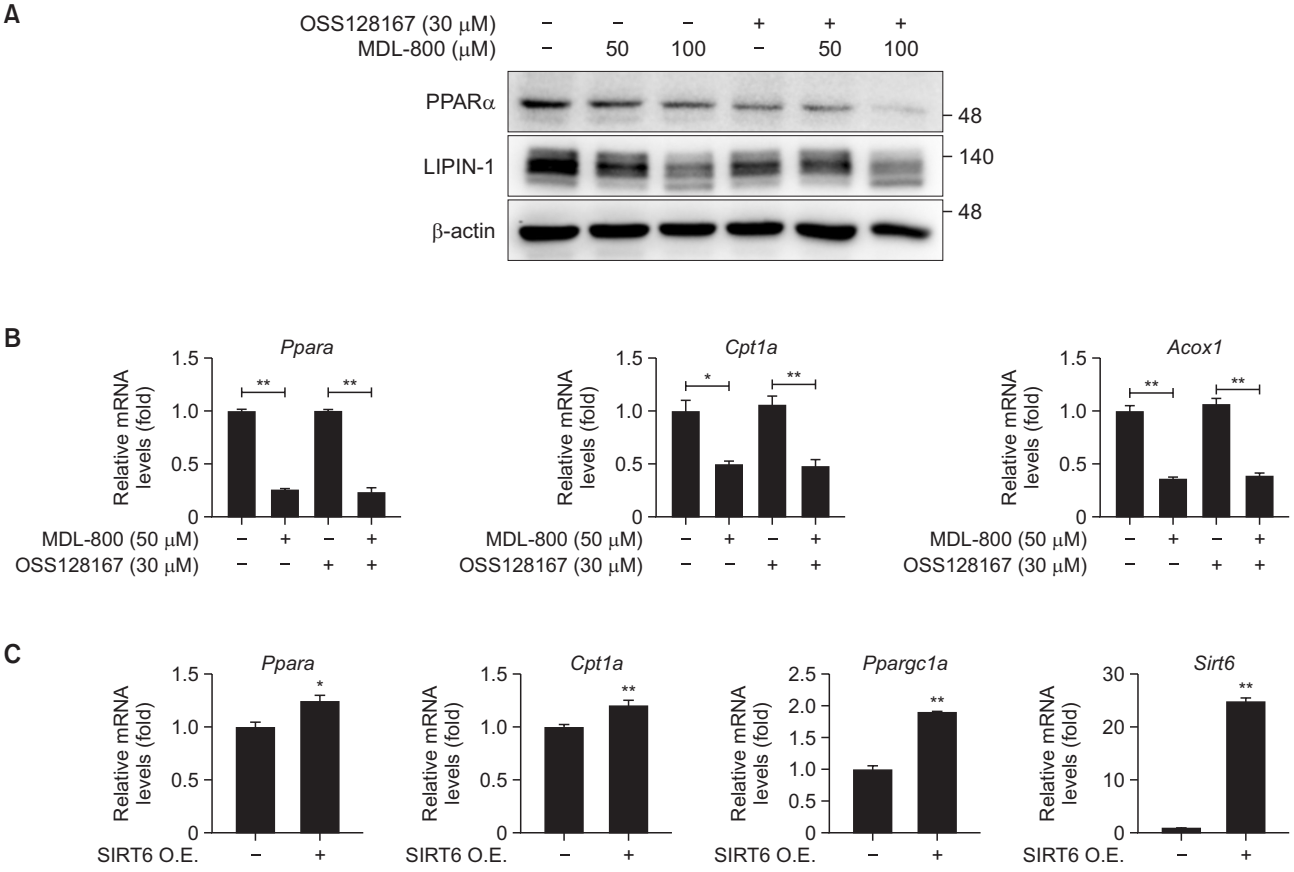

Fig. 2. MDL-800 inhibits FA oxidation-related genes independently of SIRT6 activation. (A) AML12 cells were pretreated with OSS128167 (30 μM) for 30 min or left untreated, followed by treatment with MDL-800 (50 and 100 μM) for 12 h. Total cell lysates were subjected to immunoblot analyses for PPARα and LIPIN-1. (B) AML12 cells were pretreated with OSS128167 (30 μM) for 30 min or left untreated, followed by treatment with MDL-800 (50 μM) for 12 h. RNA was extracted for RT-qPCR analysis of *Ppara*, *Cpt1a*, and *Acox1*. (C) AML12 cells were transfected with a vector overexpressing SIRT6 (1 μg) or a pcDNA3.1 control vector. After incubation for 24 h, RNA was extracted for RT-qPCR analysis of *Ppara, Cpt1a*, *Ppargc1a*, and *Sirt6*. Values represent the mean ± SEM (n=3). Statistical evaluations were performed using Student's *t*-test (**p*<0.05, ***p*<0.01).

MDL-800 activates stress kinases and enhances ROS levels in hepatocytes

To determine whether MDL-800-induced cellular stress is associated with ROS production, we measured ROS levels in AML12 cells. DCF-DA assays were performed using two methods to detect DCF fluorescence that represents intracellular ROS levels. Microscopic analyses revealed a dose-dependent increase in ROS levels following MDL-800 treatment (Fig. 4A, Supplementary Fig. 2). Consistently, quantitative analyses using a fluorescence microplate reader confirmed that MDL-800 treatment promoted ROS production in AML12 cells (Fig. 4B). Excessive ROS levels trigger cellular responses, including the activation of NRF2 and the upregulation of its downstream antioxidant genes (Attucks *et al*., 2014). In agreement with this, MDL-800 treatment increased the expression of antioxidant genes, such as *Hmox1* and *Nqo1* (Fig. 4C). Taken together, these results demonstrate that MDL-800 elevates ROS levels in hepatocytes, thereby contributing to cellular stress and PPARα inhibition.

MDL-800 inhibits PPARα and FA oxidation-related genes through ROS production

Given that MDL-800 increases ROS levels in hepatocytes and cellular stress inhibits PPARα, we investigated whether ROS plays a crucial role in mediating the suppression of PPARα and FA oxidation-related genes by MDL-800. Treatment with H_2O_2 significantly reduced the mRNA levels of *Ppara*, *Cpt1a*, and *Acox1* in AML12 cells, indicating the ability of ROS to suppress PPARα and its downstream FA oxidation-related genes (Fig. 5A). To further validate the role of ROS in MDL-800-induced inhibition of PPARα, we assessed whether this effect could be reversed by the antioxidant NAC. Pretreatment with NAC prevented the MDL-800-induced reduction in the mRNA levels of *Ppara*, *Cpt1a*, *Acox1*, and *Acadvl* (Fig. 5B), indicating that ROS production mediates the inhibitory effects of MDL-800 on PPARα and FA oxidation-related genes. Moreover, treatment with SP600125, a JNK inhibitor, mitigated the suppression of FA oxidation-related genes by MDL-800 (Fig. 5C). Taken together, these findings suggest that MDL-800 inhibits FA oxidation-related genes through ROS production and the subsequent activation of JNK signaling pathways (Fig. 6).

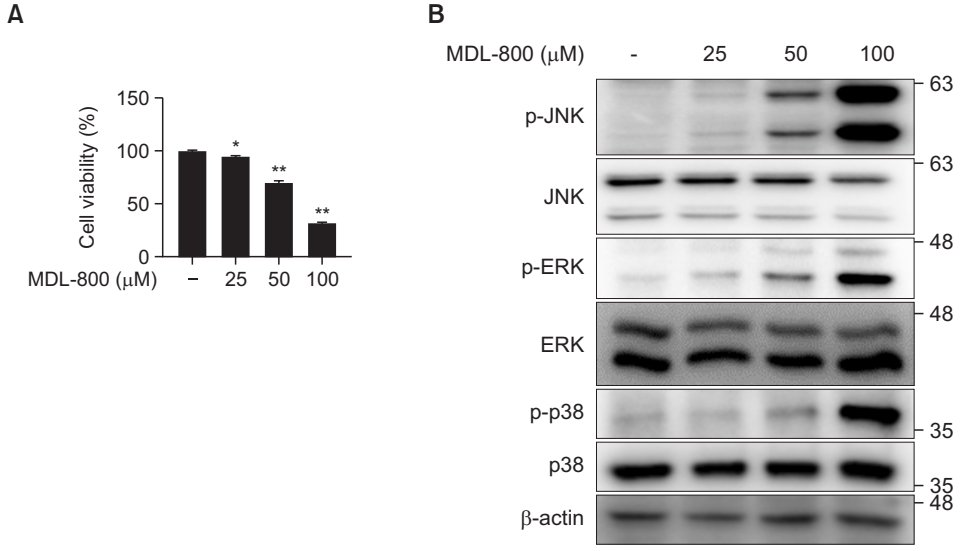

Fig. 3. MDL-800 induces cellular stress in hepatocytes. (A, B) AML12 cells were treated with MDL-800 (25, 50, and 100 μM) for 12 h and subjected to cell viability measurements using the CCK-8 assay (panel A). Whole cell lysates were analyzed via immunoblotting to assess stress kinase activation (panel B). Values represent the mean ± SEM (n=3). Statistical evaluations were performed using Student's *t*-test (**p*<0.05, ***p*<0.01).

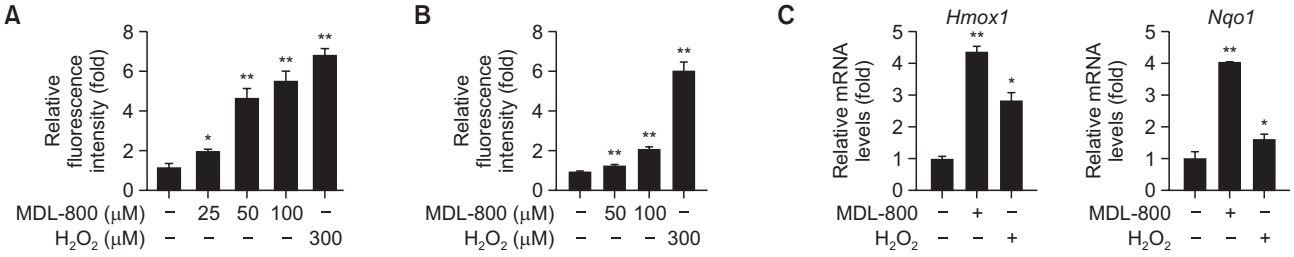

Fig. 4. MDL-800 enhances ROS levels in hepatocytes. (A, B) AML12 cells were treated with MDL-800 (various concentrations) or H_2O_2 (300 μM) for 12 h (panel A) or 6 h (panel B) and subjected to the DCF-DA assay. Cells were imaged using a fluorescent microscope, and fluorescence intensity was quantified using ImageJ (panel A). The representative images used for quantification are included in Supplementary Fig. 2. Quantitative analysis of fluorescence was also conducted using a microplate reader (panel B). (C) AML12 cells were treated with MDL-800 (50 μM) or H_2O_2 (500 μM), and RNA was extracted for RT-qPCR analysis of *Hmox1* and *Nqo1*. Values represent the mean ± SEM (n=3). Statistical evaluations were performed using Student's *t*-test (**p*<0.05, ***p*<0.01).

DISCUSSION

SIRT6 regulates a variety of biological processes related to energy metabolism, including FA oxidation. SIRT6 activation promotes FA oxidation, which has been suggested as a pharmacological strategy to ameliorate hepatic lipid accumulation and consequent lipotoxicity that exacerbates steatotic liver disease. However, in contrast to the ability of SIRT6 to activate PPARα (Naiman *et al*., 2019), the current study has demonstrated that MDL-800, a selective activator of SIRT6, inhibits PPARα and FA oxidation-related genes in hepatocytes.

The findings from the current study support the notion that MDL-800 represses PPARα in a SIRT6-independent manner. For instance, MDL-800 reduced the expression of PPARα even at concentrations where SIRT6 was activated. Moreover, the suppression of PPARα by MDL-800 persisted despite concomitant treatment with OSS128167, a SIRT6 inhibitor, further indicating that this regulatory effects is independent of SIRT6. In addition, this study has investigated the mechanistic aspects that may explain how MDL-800 inhibits PPARα and FA oxidation, providing evidence suggesting that ROS production and stress kinase activation contribute to SIRT6-independent inhibition of PPARα and FA oxidation-related genes by MDL-800. MDL-800 treatment increased cellular ROS levels and activated stress kinases in hepatocytes in addition to SIRT6 activation, and MDL-800-induced PPARα inhibition was reversed by a concomitant treatment with an antioxidant NAC or a selective JNK inhibitor SP600125. As SIRT6 overexpression in AML12 cells elevated the expression of PPARα and its target genes, SIRT6 activation by MDL-800 could potentially lead to PPARα activation; however, it is likely that MDL-800-induced ROS production overrides SIRT6-mediated PPARα activation, eventually inhibiting PPARα and its target genes.

Although the current study demonstrates that MDL-800 and H_2O_2 reduce *Ppara* mRNA levels, leading to suppressed expression of PPARα, the precise mechanism by which MDL-800 and oxidative stress decrease *Ppara* mRNA levels remains unclear. While the reduction in *Ppara* mRNA levels

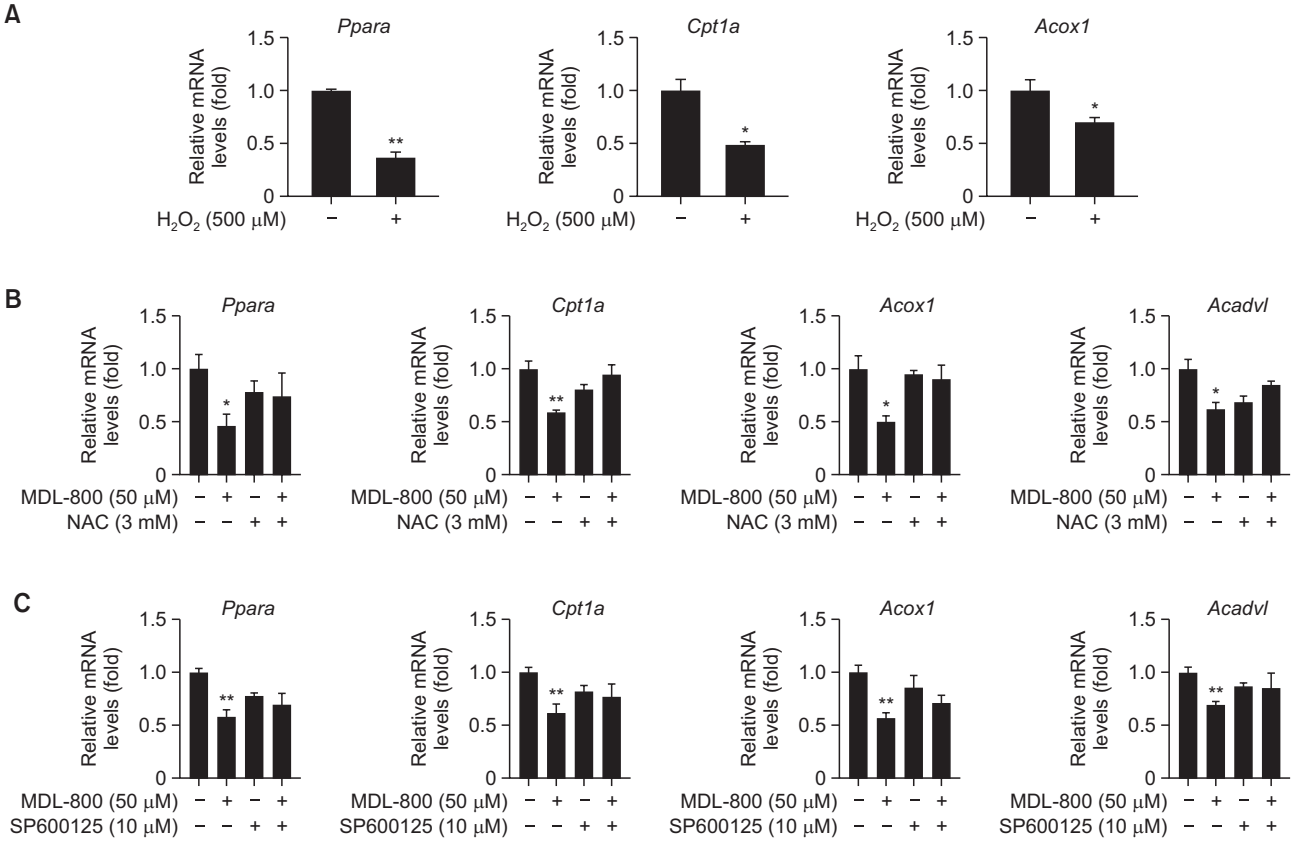

Fig. 5. MDL-800 inhibits FA oxidation-related genes via ROS production and stress kinase activation. (A) AML12 cells were treated with H_2O_2 (500 μM) for 6 h, and RNA was extracted for RT-qPCR analysis of *Ppara*, *Cpt1a*, and *Acox1*. (B, C) AML12 cells were pretreated with NAC (3 mM) or SP600125 (10 μM) for 1 h or left untreated, followed by treatment with MDL-800 (50 μM) for 12 h. RNA was extracted for RT-qPCR analysis of *Ppara*, *Cpt1a*, *Acox1*, and *Acadvl*. Values represent the mean ± SEM (n=3). Statistical evaluation was performed using Student's *t*-test (**p*<0.05, ***p*<0.01).

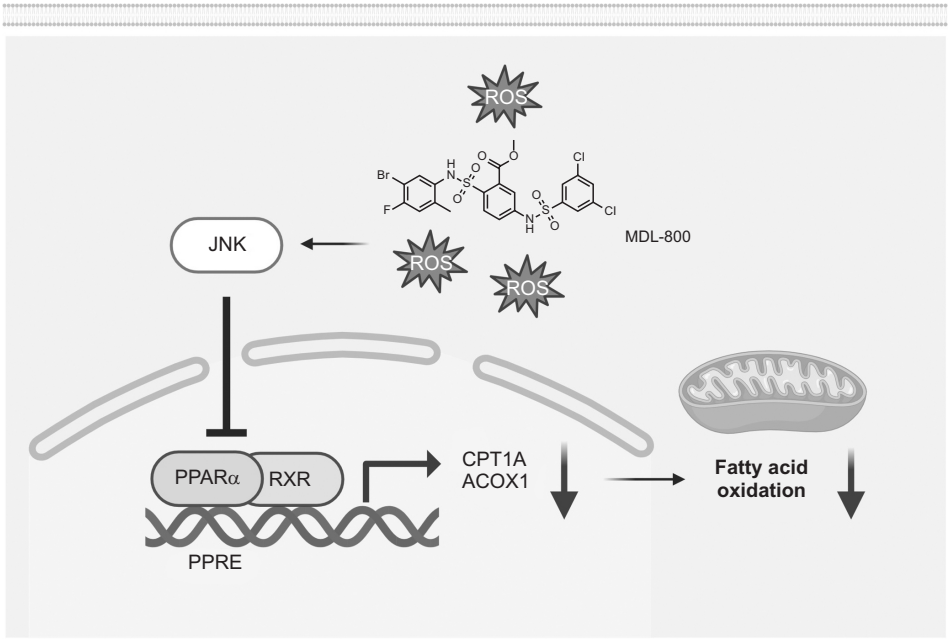

Fig. 6. Schematic representation of the inhibitory effects of MDL-800 on PPARα and FA oxidation-related genes.

could suggest transcriptional inhibition by MDL-800, other potential mechanisms, such as accelerated mRNA degradation or microRNA-mediated inhibition of *Ppara*, should also be considered. Further research is necessary to more thoroughly elucidate the detailed mechanisms underlying the regulation of *Ppara* mRNA by MDL-800.

In contrast to our findings that MDL-800 increased cellular ROS levels, Shen *et al*. reported that MDL-800 treatment attenuated ROS levels in hydrogen peroxide-treated granulosa cells (Shen *et al*., 2023). Several key discrepancies exist between their study and ours. First, while Shen *et al*. (2023) used granulosa cells, our study utilized hepatocyte lines. In addition, they tested lower concentrations of MDL-800 (2.5-10 μM), whereas we employed higher concentrations (25-50 μM). Moreover, we investigated the effect of MDL-800 alone, while Shen *et al*. (2023) tested the effect of MDL-800 in cells challenged with hydrogen peroxide. It would be interesting to explore whether MDL-800 mitigates hydrogen peroxide-induced cytotoxicity in hepatocytes, contrasting with our finding that MDL-800 exacerbates oxidative stress in untreated hepatocytes.

ROS has been shown to inhibit FA oxidation in cancer cells (Schafer *et al*., 2009), which allowed us to hypothesize that MDL-800-induced ROS production may inhibit FA oxidation; however, the precise mechanism by which ROS suppresses FA oxidation and the potential involvement of PPARα in this process remain unclear. Our study revealed that hydrogen peroxide treatment reduced the mRNA levels of *Ppara*, *Cpt1a*, and *Acox1*. The mechanism by which ROS inactivates PPARα in hepatocytes requires further investigation and remains a significant area of interest for future research.

Cancer cells require increased energy production for survival under certain conditions, such as when they lose attachment to the extracellular matrix (Carracedo *et al*., 2013). FAs are known to produce twice as much ATP as carbohydrates (Carracedo *et al*., 2013), and FA oxidation is an essential process that converts FAs into acetyl CoA, which is utilized for ATP production by Krebs cycle. The growth of cancer cells is also dependent on cytosolic NADPH levels, and FA oxidation also contributes to NADPH production as Krebs cycle produces citrate, which is involved in cytosolic production of NADPH (Pike *et al*., 2011). Schafer *et al*. demonstrated that FA oxidation supports the survival of cancer cells under metabolic stress (Schafer *et al*., 2009). Moreover, FA oxidation has been suggested as a mechanism by which cancer cells obtain resistance to immune cell-mediated cytotoxicity (Liu *et al*., 2023). Conversely, inhibition of FA oxidation has been suggested as a strategy to ameliorate various types of cancers. Samudio *et al*. reported that inhibition of FA oxidation made leukemia cells more susceptible to apoptosis induced by cancer chemotherapy (Samudio *et al*., 2010). Liu *et al*. demonstrated that abrogating FA oxidation sensitized prostate cancer cells to cellular immune cytotoxicity (Liu *et al*., 2023). In addition, lipotoxicity can be induced by the accumulation of FAs that are not processed through β-oxidation.

The anti-tumor effects of MDL-800 have been documented in several cancer types, such as HCC (Huang *et al*., 2018) and non-small cell lung cancer (Shang *et al*., 2021). However, its potential link to FA metabolism has not been explored. Our study proposes that the anti-proliferative effects of MDL-800 reported in the literature may be, at least in part, attributable to its inhibition of FA oxidation. While the SIRT6-dependent mechanisms, such as cell-cycle arrest, have been identified as contributors to the anti-proliferative activity of MDL-800, uncovering a SIRT6-independent inhibition of FA oxidation could further enhance the potential of MDL-800 as a therapeutic strategy for cancer treatment. Beyond its implications for HCC treatment, SIRT6 activation could account for various benefits against the MASLD pathogenesis. For example, SIRT6 has been shown to suppress the expression of fibrogenic genes (Maity *et al*., 2020; Zhong *et al*., 2020), and Zhang *et al*. reported that MDL-800 mitigates liver fibrosis induced by carbon tetrachloride in mice (Zhang *et al*., 2021). Further investigation is warranted to determine whether MDL-800 can alleviate MASLD-related fibrosis. However, careful consideration is necessary when developing MDL-800 for non-malignant diseases, as its established anti-proliferative effects may lead to hepatocyte cytotoxicity and exacerbate MASLD. Therefore, optimizing the dosage will be a critical challenge in tailoring MDL-800 for specific disease contexts.

CONFLICT OF INTEREST

The authors declare that they have no conflict of interest.

ACKNOWLEDGMENTS

This work was supported by a 2-Year Research Grant of Pusan National University (S.H.). Figures were created with BioRender and published with the appropriate permission.

AUTHOR CONTRIBUTIONS

Y.K. designed and conducted experiments; H.L. and Y.E.C. supported experimental procedures and analyses; S.H. supervised the project and wrote the paper.

REFERENCES

Attucks, O. C., Jasmer, K. J., Hannink, M., Kassis, J., Zhong, Z., Gupta, S., Victory, S. F., Guzel, M., Polisetti, D. R., Andrews, R., Mjalli, A. M. and Kostura, M. J. (2014) Induction of heme oxygenase I (HMOX1) by HPP-4382: a novel modulator of Bach1 activity. *PLoS One* **9**, e101044.

Carracedo, A., Cantley, L. C. and Pandolfi, P. P. (2013) Cancer metabolism: fatty acid oxidation in the limelight. *Nat. Rev. Cancer* **13**, 227-232.

Cha, J. Y. and Repa, J. J. (2007) The liver X receptor (LXR) and hepatic lipogenesis. The carbohydrate-response element-binding protein is a target gene of LXR. *J. Biol. Chem.* **282**, 743-751.

Cho, Y. E., Kim, Y., Kim, S. J., Lee, H. and Hwang, S. (2023) Overexpression of interleukin-8 promotes the progression of fatty liver to nonalcoholic steatohepatitis in mice. *Int. J. Mol. Sci.* **24**, 15489.

Chung, K. W., Cho, Y. E., Kim, S. J. and Hwang, S. (2022) Immune-related pathogenesis and therapeutic strategies of nonalcoholic steatohepatitis. *Arch. Pharm. Res.* **45**, 229-244.

Dong, X. C. (2023) Sirtuin 6-a key regulator of hepatic lipid metabolism and liver health. *Cells* **12**, 663.

Elhanati, S., Ben-Hamo, R., Kanfi, Y., Varvak, A., Glazz, R., Lerrer, B., Efroni, S. and Cohen, H. Y. (2016) Reciprocal regulation between SIRT6 and miR-122 controls liver metabolism and predicts hepatocarcinoma prognosis. *Cell Rep.* **14**, 234-242.

Finck, B. N., Gropler, M. C., Chen, Z., Leone, T. C., Croce, M. A., Har-

ris, T. E., Lawrence, J. C., Jr. and Kelly, D. P. (2006) Lipin 1 is an inducible amplifier of the hepatic PGC-1alpha/PPARalpha regulatory pathway. *Cell Metab.* **4**, 199-210.

Friedman, S. L., Neuschwander-Tetri, B. A., Rinella, M. and Sanyal, A. J. (2018) Mechanisms of NAFLD development and therapeutic strategies. *Nat. Med.* **24**, 908-922.

Geng, Y., Faber, K. N., de Meijer, V. E., Blokzijl, H. and Moshage, H. (2021) How does hepatic lipid accumulation lead to lipotoxicity in non-alcoholic fatty liver disease? *Hepatol. Int.* **15**, 21-35.

Huang, Z., Zhao, J., Deng, W., Chen, Y., Shang, J., Song, K., Zhang, L., Wang, C., Lu, S., Yang, X., He, B., Min, J., Hu, H., Tan, M., Xu, J., Zhang, Q., Zhong, J., Sun, X., Mao, Z., Lin, H., Xiao, M., Chin, Y. E., Jiang, H., Xu, Y., Chen, G. and Zhang, J. (2018) Identification of a cellularly active SIRT6 allosteric activator. *Nat. Chem. Biol.* **14**, 1118-1126.

Hwang, S., Hartman, I. Z., Calhoun, L. N., Garland, K., Young, G. A., Mitsche, M. A., McDonald, J., Xu, F., Engelking, L. and DeBose-Boyd, R. A. (2016) Contribution of accelerated degradation to feedback regulation of 3-hydroxy-3-methylglutaryl coenzyme A reductase and cholesterol metabolism in the liver. *J. Biol. Chem.* **291**, 13479-13494.

Hwang, S., He, Y., Xiang, X., Seo, W., Kim, S. J., Ma, J., Ren, T., Park, S. H., Zhou, Z., Feng, D., Kunos, G. and Gao, B. (2020a) Interleukin-22 ameliorates neutrophil-driven nonalcoholic steatohepatitis through multiple targets. *Hepatology* **72**, 412-429.

Hwang, S., Wang, X., Rodrigues, R. M., Ma, J., He, Y., Seo, W., Park, S. H., Kim, S. J., Feng, D. and Gao, B. (2020b) Protective and detrimental roles of p38α mitogen-activated protein kinase in different stages of nonalcoholic fatty liver disease. *Hepatology* **72**, 873-891.

Jiang, H., Khan, S., Wang, Y., Charron, G., He, B., Sebastian, C., Du, J., Kim, R., Ge, E., Mostoslavsky, R., Hang, H. C., Hao, Q. and Lin, H. (2013) SIRT6 regulates TNF-α secretion through hydrolysis of long-chain fatty acyl lysine. *Nature* **496**, 110-113.

Kim, H. S., Xiao, C., Wang, R. H., Lahusen, T., Xu, X., Vassilopoulos, A., Vazquez-Ortiz, G., Jeong, W. I., Park, O., Ki, S. H., Gao, B. and Deng, C. X. (2010) Hepatic-specific disruption of SIRT6 in mice results in fatty liver formation due to enhanced glycolysis and triglyceride synthesis. *Cell Metab.* **12**, 224-236.

Kwon, Y. S., Cho, Y. E., Kim, Y., Koh, M. and Hwang, S. (2024) Dimethyloxalylglycine suppresses SREBP1c and lipogenic gene expressions in hepatocytes independently of HIF1A. *Curr. Issues Mol. Biol.* **46**, 2386-2397.

Liu, Z., Liu, W., Wang, W., Ma, Y., Wang, Y., Drum, D. L., Cai, J., Blevins, H., Lee, E., Shah, S., Fisher, P. B., Wang, X., Fang, X., Guo, C. and Wang, X. Y. (2023) CPT1A-mediated fatty acid oxidation confers cancer cell resistance to immune-mediated cytolytic killing. *Proc. Natl. Acad. Sci. U. S. A.* **120**, e2302878120.

Maity, S., Muhamed, J., Sarikhani, M., Kumar, S., Ahamed, F., Spurthi, K. M., Ravi, V., Jain, A., Khan, D., Arathi, B. P., Desingu, P. A. and Sundaresan, N. R. (2020) Sirtuin 6 deficiency transcriptionally upregulates TGF-β signaling and induces fibrosis in mice. *J. Biol. Chem.* **295**, 415-434.

Mehal, W. (2023) Mechanisms of liver fibrosis in metabolic syndrome. *eGastroenterology* **1**, e100015.

Moon, Y. J., Zhang, Z., Bang, I. H., Kwon, O. K., Yoon, S. J., Kim, J. R., Lee, S., Bae, E. J. and Park, B. H. (2019) Sirtuin 6 in preosteoclasts suppresses age- and estrogen deficiency-related bone loss by stabilizing estrogen receptor α. *Cell Death Differ.* **26**, 2358-2370.

Moreno, M., Lombardi, A., Silvestri, E., Senese, R., Cioffi, F., Goglia, F., Lanni, A. and de Lange, P. (2010) PPARs: nuclear receptors controlled by, and controlling, nutrient handling through nuclear and cytosolic signaling. *PPAR Res.* **2010**, 435689.

Naiman, S., Huynh, F. K., Gil, R., Glick, Y., Shahar, Y., Touitou, N., Nahum, L., Avivi, M. Y., Roichman, A., Kanfi, Y., Gertler, A. A., Doniger, T., Ilkayeva, O. R., Abramovich, I., Yaron, O., Lerrer, B., Gottlieb, E., Harris, R. A., Gerber, D., Hirschey, M. D. and Cohen, H. Y. (2019) SIRT6 promotes hepatic beta-oxidation via activation of PPARα. *Cell Rep.* **29**, 4127-4143.e4128.

Pike, L. S., Smift, A. L., Croteau, N. J., Ferrick, D. A. and Wu, M. (2011) Inhibition of fatty acid oxidation by etomoxir impairs NADPH production and increases reactive oxygen species resulting in ATP depletion and cell death in human glioblastoma cells. *Biochim. Biophys. Acta* **1807**, 726-734.

Samudio, I., Harmancey, R., Fiegl, M., Kantarjian, H., Konopleva, M., Korchin, B., Kaluarachchi, K., Bornmann, W., Duvvuri, S., Taegtmeyer, H. and Andreeff, M. (2010) Pharmacologic inhibition of fatty acid oxidation sensitizes human leukemia cells to apoptosis induction. *J. Clin. Invest.* **120**, 142-156.

Sanyal, A. J. (2019) Past, present and future perspectives in nonalcoholic fatty liver disease. *Nat. Rev. Gastroenterol. Hepatol.* **16**, 377-386.

Schafer, Z. T., Grassian, A. R., Song, L., Jiang, Z., Gerhart-Hines, Z., Irie, H. Y., Gao, S., Puigserver, P. and Brugge, J. S. (2009) Antioxidant and oncogene rescue of metabolic defects caused by loss of matrix attachment. *Nature* **461**, 109-113.

Schultz, J. R., Tu, H., Luk, A., Repa, J. J., Medina, J. C., Li, L., Schwendner, S., Wang, S., Thoolen, M., Mangelsdorf, D. J., Lustig, K. D. and Shan, B. (2000) Role of LXRs in control of lipogenesis. *Genes Dev.* **14**, 2831-2838.

Shang, J. L., Ning, S. B., Chen, Y. Y., Chen, T. X. and Zhang, J. (2021) MDL-800, an allosteric activator of SIRT6, suppresses proliferation and enhances EGFR-TKIs therapy in non-small cell lung cancer. *Acta Pharmacol. Sin.* **42**, 120-131.

Shen, C., Jiang, Y., Lin, J., He, Y., Liu, Y. and Fang, D. (2023) SIRT6 reduces the symptoms of premature ovarian failure and alleviates oxidative stress and apoptosis in granulosa cells by degrading p66SHC via H3K9AC. *Gynecol. Endocrinol.* **39**, 2250003.

Shi, M. Y., Bang, I. H., Han, C. Y., Lee, D. H., Park, B. H. and Bae, E. J. (2020) Statin suppresses sirtuin 6 through miR-495, increasing FoxO1-dependent hepatic gluconeogenesis. *Theranostics* **10**, 11416-11427.

Tasselli, L., Zheng, W. and Chua, K. F. (2017) SIRT6: novel mechanisms and links to aging and disease. *Trends Endocrinol. Metab.* **28**, 168-185.

Vernia, S., Cavanagh-Kyros, J., Garcia-Haro, L., Sabio, G., Barrett, T., Jung, D. Y., Kim, J. K., Xu, J., Shulha, H. P., Garber, M., Gao, G. and Davis, R. J. (2014) The PPARα-FGF21 hormone axis contributes to metabolic regulation by the hepatic JNK signaling pathway. *Cell Metab.* **20**, 512-525.

Wong, V. W., Ekstedt, M., Wong, G. L. and Hagström, H. (2023) Changing epidemiology, global trends and implications for outcomes of NAFLD. *J. Hepatol.* **79**, 842-852.

Wu, X., Liu, H., Brooks, A., Xu, S., Luo, J., Steiner, R., Mickelsen, D. M., Moravec, C. S., Jeffrey, A. D., Small, E. M. and Jin, Z. G. (2022) SIRT6 mitigates heart failure with preserved ejection fraction in diabetes. *Circ. Res.* **131**, 926-943.

Xu, X., So, J. S., Park, J. G. and Lee, A. H. (2013) Transcriptional control of hepatic lipid metabolism by SREBP and ChREBP. *Semin. Liver Dis.* **33**, 301-311.

You, Y. and Liang, W. (2023) SIRT1 and SIRT6: the role in aging-related diseases. *Biochim. Biophys. Acta Mol. Basis Dis.* **1869**, 166815.

Zhang, J., Li, Y., Liu, Q., Huang, Y., Li, R., Wu, T., Zhang, Z., Zhou, J., Huang, H., Tang, Q., Huang, C., Zhao, Y., Zhang, G., Jiang, W., Mo, L., Zhang, J., Xie, W. and He, J. (2021) Sirt6 alleviated liver fibrosis by deacetylating conserved lysine 54 on Smad2 in hepatic stellate cells. *Hepatology* **73**, 1140-1157.

Zhong, X., Huang, M., Kim, H. G., Zhang, Y., Chowdhury, K., Cai, W., Saxena, R., Schwabe, R. F., Liangpunsakul, S. and Dong, X. C. (2020) SIRT6 protects against liver fibrosis by deacetylation and suppression of SMAD3 in hepatic stellate cells. *Cell. Mol. Gastroenterol. Hepatol.* **10**, 341-364.

Zhu, C., Huang, M., Kim, H. G., Chowdhury, K., Gao, J., Liu, S., Wan, J., Wei, L. and Dong, X. C. (2021) SIRT6 controls hepatic lipogenesis by suppressing LXR, ChREBP, and SREBP1. *Biochim. Biophys. Acta Mol. Basis Dis.* **1867**, 166249.